

# Multi-scale scanning tunneling microscopy imaging of self-organized regioregular poly(3-hexylthiophene) films

B. Grévin,<sup>a)</sup> P. Rannou, R. Payerne, A. Pron, and J. P. Travers

Laboratoire de Physique des Métaux Synthétiques UMR5819-SPRAM (CEA-CNRS Université Grenoble I), DRFMC CEA-Grenoble, 17 rue des Martyrs 38054 Grenoble Cedex 9, France

(Received 8 November 2002; accepted 23 January 2003)

Two-dimensional self-organized poly(3-hexylthiophene) films on highly oriented pyrolytic graphite have been probed at the solid/substrate interface by scanning tunneling microscopy (STM). Structural morphology and typical polymer conformations are visualized and discussed from mesoscopic to nanoscopic scales, including mesoscopic assembly of polycrystals, crystalline monodomain orientations and sizes, grain boundaries, chain folds, and other conformational features. STM estimation of the average chain length is in remarkably good agreement with that derived from size-exclusion chromatography. The multiscale analysis supports a picture where heterogeneities exist at different length scales. © 2003 American Institute of Physics.

[DOI: 10.1063/1.1561435]

## I. INTRODUCTION

In view of the recent developments of polymer electronics, detailed elucidation of structural order at different length scales in self-organized  $\pi$ -conjugated semi-conducting polymers is of crucial importance. Poly(3-alkylthiophene)s (abbreviated as P3ATs) are very well suited for this type of study. New methods of their synthesis developed in the past few years,<sup>1–4</sup> resulted in the preparation of regiochemically well-defined P3ATs with more than 99% of head-to-tail coupling (so-called regioregular HT-HT P3ATs). The highly regular chain structure of P3ATs facilitates their self-organization into two-dimensional sheets via interchain stacking. Furthermore, solution processibility of these polymers enables easy preparation of thin solid films using different types of solution casting techniques. P3ATs have been recently tested as semi-conducting components of polymer field-effect transistors<sup>5–8</sup> (FETs) because their ordered supramolecular organization results in improved electrical transport properties. For example, in FETs made of regioregular poly(3-hexylthiophene) (P3HT), field-effect mobilities as high as  $0.1 \text{ cm}^2 \text{ V}^{-1} \text{ s}^{-1}$  have been achieved.<sup>6,7</sup>

The microstructure of solution-processed P3AT films has been intensively studied by x-ray diffraction<sup>9–12</sup> (XRD), and valuable information about film anisotropy and the typical size of crystalline domains have been obtained (crystalline coherence length have been reported in the range 8–13 nm for P3HT<sup>10,11</sup>). Nonetheless, the mesoscopic structure of P3AT films is generally expected to be more complex than a simple polycrystal, and it probably consists of polycrystalline domains embedded in a disordered/amorphous matrix.<sup>11</sup> Besides, on a more local scale, P3ATs may present structural heterogeneities such as paracrystallinity and/or disorder.<sup>9</sup> Such a complex structure with heterogeneities at different scales can give rise to various effects or properties, whose

origin may be difficult to identify when performing a global measurement on the polymer. As an example, XRD peak width narrowing has been associated with an increase in crystallite size<sup>10</sup> when heating poly(3-octylthiophene) films, whereas the same effect measured on poly(3-dodecylthiophene) has been attributed to fluctuations and variations in microscopic heterogeneities.<sup>9</sup>

With regard to this structural complexity, an interesting alternative consists in studying the polymer microstructure by using local probes.<sup>13,14</sup> Scanning tunneling microscopy (STM) has been applied to the study of regiorandom<sup>15,16</sup> and regioregular semiconducting poly(3-alkylthiophene) macromolecules on Au(111),<sup>16</sup> highly oriented pyrolytic graphite<sup>17,18</sup> (HOPG) and Cu(111) (Ref. 19) surfaces. Electrostatic force microscopy<sup>20</sup> (EFM) measurements have also been recently reported for doped (conducting) poly(thiophene) monolayers. So far, two-dimensional (2D) ordered structures resulting from self-organization of semiconducting P3AT, have only been imaged by STM at the solution/substrate (HOPG) interface.<sup>17,18</sup> In these conditions, the molecular alignment may be considered as an equilibrium state between adsorbed and solution states.<sup>14</sup> In this last study,<sup>17</sup> a direct visualization of the conjugated polymer inside ordered domains was achieved, and local parameters such as chain-to-chain packing and chain folding were clearly resolved.

In this paper, we report a multi-scale (from  $\mu\text{m}$  to sub-nanometer) STM analysis at the solid/substrate interface of a “dry” regioregular (HT-HT>99%) P3HT film deposited on HOPG (by casting from chloroform solution). Structural heterogeneities and/or typical polymer conformations are visualized and discussed at each scale: (i) polycrystalline/amorphous domains and surface coverage on mesoscopic scale, (ii) sizes, relative orientations of monodomains, and grain boundaries (GB) inside polycrystals, (iii) local polymer conformations (chain folds and molecular weight analysis), and (iv) intrachain conformations (*cis* vs *trans*). Thus, the

<sup>a)</sup> Author to whom correspondence should be addressed. Electronic address: bgrevin@cea.fr

presented research demonstrates the versatility of STM as a tool capable of probing self-assembled  $\pi$ -conjugated polymer aggregations of a complex nature at different length scales.

## II. EXPERIMENT

Regioregular (HT-HT>99%) poly(3-hexylthiophene-2,5-diyl) (P3HT) was purchased from Aldrich. Analytical size-exclusion chromatography (SEC) characterization of P3HT was performed on a 1100 HP Chemstation equipped with a 300 $\times$ 7.5 mm PLgel Mixed-D 5  $\mu$ m/10<sup>4</sup> Å column (Polymer Labs), a diode array uv-visible detector (DAD), and a refractive index (RI) detector. The column temperature and the flow rate were fixed to 313 K and 1 ml min<sup>-1</sup>, respectively. The calibration curve was built using 10 polystyrene (PS) narrow standards (S-M2-10\* kit from Polymer Labs). Two runs of 20  $\mu$ l injection of about 2.5 mg ml<sup>-1</sup> P3HT HPLC-grade THF (Acros) dilute solutions were typically analyzed for each sample with a uv-visible detection at 420 nm.

5  $\mu$ l of a 2.5  $\mu$ g ml<sup>-1</sup> solution of P3HT in CHCl<sub>3</sub> (Merck) was drop-cast on freshly cleaved highly oriented pyrolytic graphite (HOPG, grade ZYH, mosaic spread 3.5  $\pm$  1.5°, Adv. Ceramics Co.). According to visual inspection, complete evaporation of the solvent was achieved in a few seconds. To ensure complete removal of the solvent, however, STM experiments were carried out several hours after the film deposition.

STM measurements were performed with W tips in ambient conditions using an Omicron CryoSXM STM head, adapted with a homemade vibration isolation system (including spring suspension and eddy-current damping). The scanner tube was calibrated with a set of atomically resolved HOPG images (at room temperature). All images were obtained with a sample bias voltage  $V_S$  of 0.8 V and a tunneling current  $I_t$  of 0.8 nA in the constant current mode.

No treatment other than slope subtraction was applied to the images, with the exception of Fig. 4(b) for which a fast Fourier transform (FFT) filtering was used to attenuate high-frequency noise. Error bars on topographic distances deduced from line profiles were estimated according to the image pitch. For profiles in reciprocal space obtained from FFT images, we considered an error of at least 1/ $D$ ,  $D$  being the size of the topographic image from which the FFT was calculated. FFT images correspond to the module of 2D FFT (displayed in linear scale), calculated by using the WSXM software.<sup>30</sup>

## III. RESULTS

### A. Mesoscopic scale

Figure 1(a) presents a typical STM image, recorded on a mesoscopic scale (typical length 1  $\mu$ m). It reveals bright islands, spanning over distances up to several hundreds of nanometers. Following images [Fig. 1(b) and forthcoming figures] on smaller scales directly show that these areas are formed by ordered polycrystalline domains. Between these organized areas, no clear image of the underlying substrate was obtained on the mesoscopic scale. Moreover, on smaller

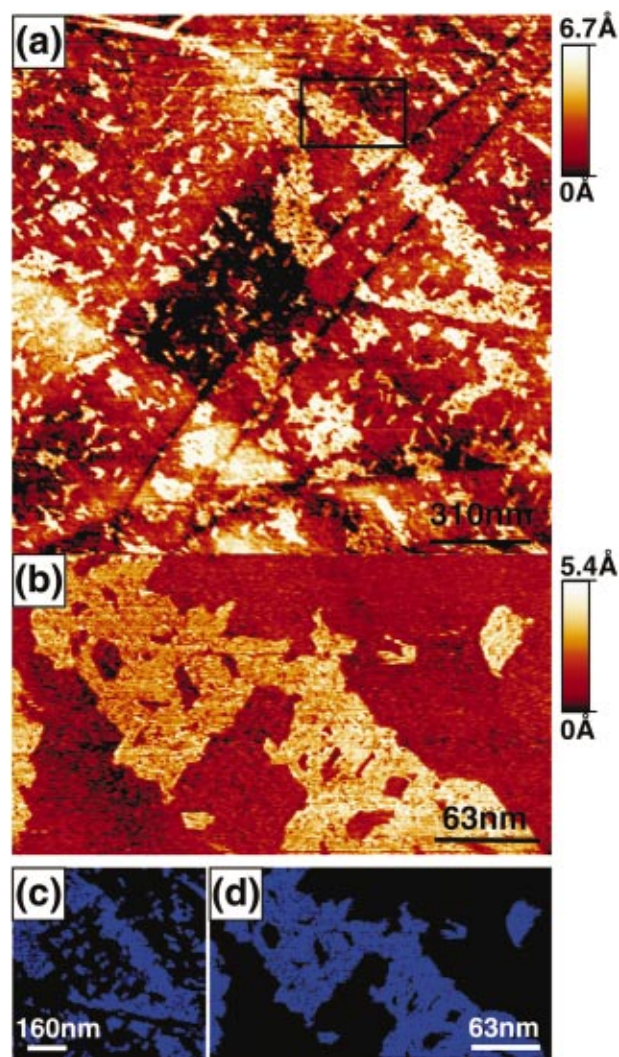


FIG. 1. (Color) (a) 1.5 $\times$ 1.5  $\mu$ m (pitch=6 nm) STM image showing mesoscopic ordering of P3HT on HOPG. The bright islands are formed by ordered polycrystalline areas, and the brown areas are partially covered by amorphous P3HT (see text). (b) 314 $\times$ 175 nm (pitch=0.5 nm) STM image of P3HT polycrystals, corresponding to the area delimited by a black rectangle in part (a). (c) Shape analysis in an 782 $\times$ 770 nm area (surface=0.602  $\mu$ m<sup>2</sup>) extracted from part (a). 27% of the surface is flooded by crystallites. (d) Shape analysis of part (b) (314 $\times$ 175 nm, surface=0.055  $\mu$ m<sup>2</sup>). 40% of the surface is flooded by crystallites.

scales (see Figs. 2, 3, and 4), the obtained images suggest that these remaining areas are at least partially covered by amorphous polymer. This seems particularly true when considering Fig. 4(a), where disordered areas are clearly visible.

The  $z$  corrugation between ordered areas (bright) and others never exceeds 2 Å. One possible explanation is that ordered areas (with better semi-conducting properties) give rise to an increased tunneling current, resulting in higher  $z$  values (in constant current mode).

A remarkable feature is that ordered patches seem to be disconnected on a  $\mu$ m scale. By performing shape analysis on various parts of several mesoscopic images [an example is shown in Fig. 1(c)], we conclude that less than 30% of the surface is covered by crystalline domains. To get a clear percolation of crystalline objects over the image, one needs to reduce the scale. This point is illustrated by Fig. 1(d),

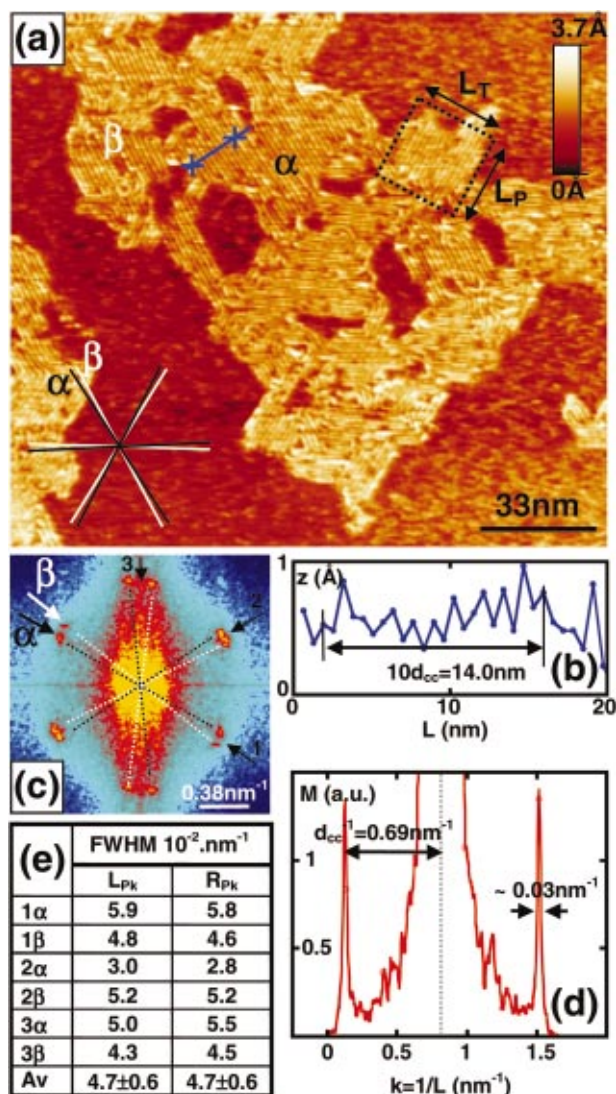


FIG. 2. (Color) (a)  $164 \times 147$  nm STM image (pitch=0.5 nm, resolution for FFT  $\approx 1/150 \approx 0.006 \text{ nm}^{-1}$ ), showing P3HT ordering on a submicron scale. The black and white stars indicate threefold symmetry directions for polymer ordering, with a misfit angle between  $\alpha$ -type and  $\beta$ -type domains (two domains are directly labeled in the image). A black dotted square shows a monodomain with dimensions  $L_P \approx L_T \approx 20$  nm (see text). (b) Topographic profile [blue line in part (a)]: the chain-to-chain distance is  $d_{cc} = 1.40 \pm 0.05$  nm. (c) FFT of topographic image. Threefold symmetry directions are labeled 1, 2, and 3.  $\alpha$  and  $\beta$  orientations are indicated by black and white arrows and dotted lines. (d) Profile (FFT module) along the  $2\alpha$  direction in an FFT image. The chain-to-chain distance deduced from the FFT profile is  $d_{cc} = 1.44 \pm 0.01$  nm ( $1/d_{cc} = 0.695 \pm 0.006 \text{ nm}^{-1}$ ). (e) Full width at half maxima (FWHM) of FFT peaks ( $L_{PK}$  and  $R_{PK}$  stand, respectively, for left and right peaks). The transverse coherence length is  $L_C = 21 \pm 3$  nm (average value from left and right peaks FWHMs in all directions,  $\langle \text{FWHM} \rangle_{av} = 1/L_C = 0.047 \pm 0.006 \text{ nm}^{-1}$ ).

which displays connected polycrystalline domains through the main section of the image (surface coverage is 40% in this case). Note that the total surfaces of images 1(c) and 1(d) differ by more than an order of magnitude (see Fig. 1 caption).

## B. Polycrystals

Let us now focus on Fig. 2(a), which displays the structure of a polycrystalline domain on a sub- $\mu\text{m}$  scale (typical

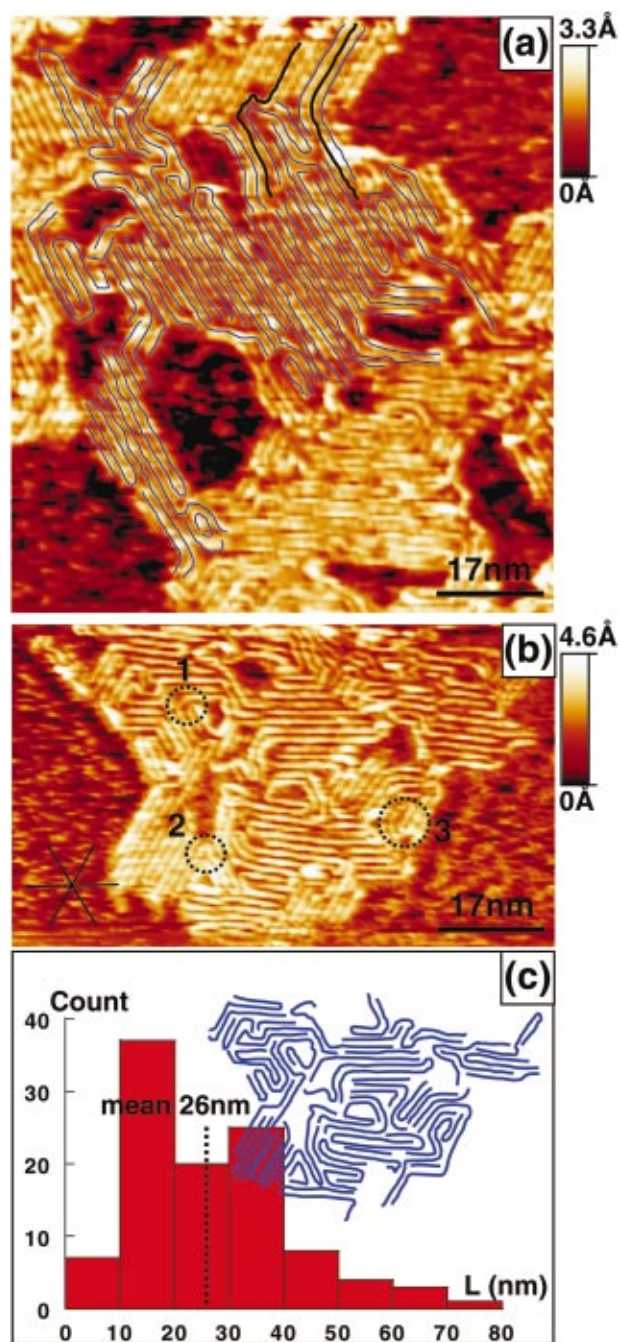


FIG. 3. (Color) (a)  $82.7 \times 91.3$  nm STM image (pitch=0.5 nm), showing a magnified image corresponding to the domain labeled  $\alpha$  in Fig. 2(a). Chain contours are underlined by blue lines. Examples of chains connecting two different monodomains are signaled by black contours. (b)  $87 \times 51.1$  nm STM image (pitch=0.5 nm) of another area. The dotted circles labeled 1, 2, and 3 indicate, respectively,  $120^\circ$ ,  $60^\circ$ , and  $360^\circ$  folds. Chain contours are displayed as an inset in the following panel. (c) Histogram of chain length distribution built by using the chain contours determined from parts (a) and (b).

length 100 nm). Domains with regular alignment of chains are clearly visible, following a three-fold symmetry orientation induced by epitaxial effects on HOPG,<sup>17</sup> due to preferential interactions between alkyl sidechains and the substrate<sup>21</sup> (hexyl sidechains are oriented along the graphite main axis). This symmetry is clearly identified from the hexagonal pattern in the FFT image [Fig. 2(c)]. Interestingly,

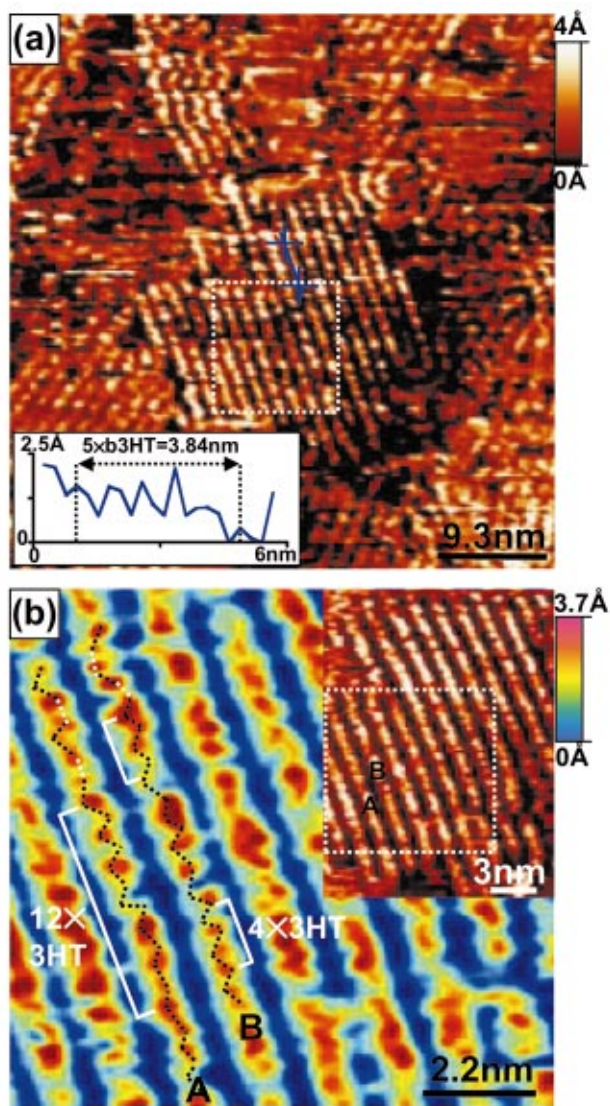


FIG. 4. (Color) (a)  $46.7 \times 48$  nm STM image (pitch =  $2 \text{ \AA}$ ), showing ordered domains and disordered/amorphous areas. The white dotted square indicates the location of part (b). Inset: topographic profile taken along the blue line in part (a), with modulations corresponding to b3HT (b3HT =  $7.7 \pm 0.4 \text{ \AA}$ ) repeating distance (see scheme 1) (b) main:  $11.2 \times 10.8$  nm (pitch =  $0.9 \text{ \AA}$ ) STM image showing the chain conformation with submolecular resolution (N.B.: this image is enlarged from that displayed as the inset). Straight white lines correspond to multiples of the 3HT repeating distance (3HT =  $3.8 \text{ \AA} \pm 0.1 \text{ \AA}$ ). Dotted lines show possible intrachain conformations of thiophene units within two chains labeled A and B (trans in black, cis in white). (b) Inset:  $15.2 \times 20.5$  nm (pitch =  $0.9 \text{ \AA}$ ) STM image. The white dotted square indicates the location of the main image.

one can remark on the presence of a misfit angle ( $\approx 6^\circ$ ) between some domains labeled  $\alpha$  and  $\beta$  that may eventually be attributed to a structural defect in the underlying substrate (such as substrate mosaicity). This feature can be seen by a careful inspection of chain alignment directions in the topographic image. It appears more directly when considering the FFT image, where spots of the hexagonal pattern are double in each of the three-fold symmetry directions.

The simultaneous analysis in direct and reciprocal spaces allows a precise estimation of the chain-to-chain distance. The profile lines taken in both topographic [Fig. 2(b)] and FFT images [Fig. 2(d)] give within the error bars the

same chain-to-chain close-packed distance,  $d_{cc} \sim 1.4$  nm.

Furthermore, the average monodomain size can be directly determined by analyzing shapes of several monodomains in topographic images. For large polycrystalline areas [analysis of 17 monodomain shapes from Fig. 1(b)], we found similar average values for the domain size in the parallel ( $L_P \approx 19$  nm, along the  $\pi$ -conjugated backbone) and in the transverse direction [ $L_T \approx 20$  nm, perpendicular to the  $\pi$ -conjugated backbone; see Fig. 2(a)]. A monodomain with a 20 nm size in both directions is indicated in Fig. 2(a).

In the case of the average size in transverse direction, an alternative method consists in measuring the FFT peaks full width at half maximum (FWHM), which gives access to a transverse coherence length  $L_C$  ( $1/\text{FWHM} = L_C$ ). This procedure is valid, because the size of the topographic image largely exceeds the dimensions of monodomains.

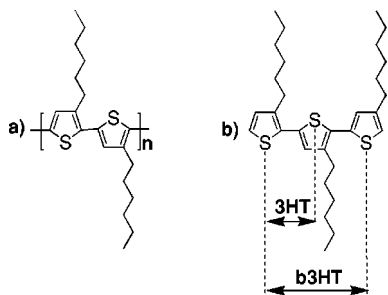
The average value obtained from FFT profiles in the three main symmetry directions is  $L_C = 21 \pm 3$  nm [see Figs. 2(d) and 2(e)]. This result is fully consistent with the value previously obtained from the topographic shape analysis ( $L_T \approx 20$  nm).

### C. Domain interfaces, folds, and molecular weight

In this section, we will discuss the chain conformation on a more local scale (inside crystalline domains and at their boundaries). In two images [Figs. 3(a) and 3(b)], we have tentatively proposed contours delimiting single polymer chains, with the aim to identify folds and to perform a direct estimation of the polymer molecular weight. To minimize possible errors, this was done only in parts of the images where polymer paths could easily be identified. On both images, we obtained almost identical average chain length values (26 nm averaged from 58 chains and 25.5 nm averaged from 48 chains for Figs. 3(a) and 3(b), respectively).

The histogram of chain length distribution deduced from contours (sum of both images data) is given in Fig. 3(c). The mean value is  $L_{chain} = 26$  nm, which is consistently larger than the aforementioned average monodomain size in parallel direction ( $L_P \approx 19$  nm). Indeed, one notices that in both images domains with different orientations are interconnected by folded chains. Some of these interdomain chains are indicated in Fig. 3(a). Thus, chain length must be on average higher than  $L_P$ . Moreover, this points to the absence of well-delimited interfaces between the domains. In that sense, it is difficult to define GBs from the images.

Next, we focus on the comparison between STM images and analytical size-exclusion chromatography (SEC) results. SEC characterization of P3HT shows an average molecular weight (in weight)  $M_w$  of 53.4 kDa (eq. PS) and a polydispersity index of 2.1. However, it is known that molecular weights of  $\pi$ -conjugated polymers are largely inflated when obtained from SEC characterization based on PS standards.<sup>22–24</sup> A recent study on P3HT<sup>24</sup> has shown that an overestimation factor of 2.0 should be taken into account when determining the absolute  $M_w$  from SEC results. With the molecular weight of a 3-hexylthiophene unit ( $M_w = 168.3 \text{ g mol}^{-1}$ ) and the polydispersity index of 2.1, calculation leads to uncorrected and corrected average degrees of poly-



SCHEME 1. (a) P3HT: Regioregular HT-HT poly(3-hexylthiophene-2,5-diyl). (b) Definition of 3HT and b3HT distances (sulfur-sulfur distances in diad and triad, respectively), as used in the text and in Fig. 4.

merization in number ( $DP_n$ ) of about 151 and 76, respectively. If one considers a distance of  $3.8 \text{ \AA}$  for a “3-hexylthiophene unit” (see the 3HT distance deduced from our STM measurements in Sec. III D, Scheme 1, and Fig. 4), one obtains an average chain length  $L_{SEC}$  of about 29 nm (using the corrected  $DP_n$ ). This value is in good agreement with the one obtained from STM imaging (contour length analysis,  $L_{chain} = 26 \text{ nm}$ ).

Last, we can use chain contours to perform a statistical analysis of folds. It appears that chain folding occurs following in majority the three-fold epitaxy-induced symmetry (60% of folds with  $120^\circ$  angles and 10% of folds with  $60^\circ$  angles). Other folds are regular with angle of  $360^\circ$  (20%), or unclassified ones (10% of folds with apparent angles different from  $60^\circ$ ,  $120^\circ$ , or  $360^\circ$ ). Some typical folds are indicated in Fig. 3(b).

#### D. Intrachain modulations

The smallest scale in analysis is reached with Fig. 4, where images with a subnanometer resolution are displayed. Figure 4(a) shows a monodomain in its center, surrounded by other domains and in some parts by more disordered areas. We believe that this image can be taken as a direct experimental evidence in favor of a heterogeneous picture involving the coexistence of ordered and disordered domains.

Note also that at this scale, modulations along chains ( $\pi$ -conjugated backbone direction) are revealed. Topographic profile lines [insert in Fig. 4(a)] show that these periodicities correspond to b3HT distances (sulfur-sulfur distance in a triad) as depicted in Scheme 1, with a measured value of  $b3HT = 7.7 \pm 0.5 \text{ \AA}$ .

Even more detailed structural features can be revealed at a smaller scale [Fig. 4(b) and insert: high resolution image obtained in the central monodomain aforementioned]. In many parts of Fig. 4(b), modulations correspond to 3HT distances (sulfur-sulfur distance in a diad; see Scheme 1). Measurements of several modulations length give an average value  $3HT = 3.8 \pm 0.08 \text{ \AA}$  ( $b3HT = 7.6 \pm 0.2 \text{ \AA}$ ).

Within the resolution of this image, we tentatively propose possible intrachain conformations for 3-hexylthiophene units [*trans* versus *cis*, respectively represented by black and white dotted lines in Fig. 4(b)]. Due to resolution limits (pitch of the image is  $0.9 \text{ \AA}$ ), we adopted the following procedure. Distances corresponding to multiples of the

3-hexylthiophene unit in all-*trans* geometry (white full lines in the image) were compared to distances between spots along the chain axis. An additional constraint was considered by taking into account interdigitation between adjacent chains (an intrachain topology must be consistent with that of its neighbor). As a result, we found that chain modulations were consistent with all-*trans* geometry in most part of the image, with the exception of the upper left corner of the image, where possible *cis* conformations are tentatively proposed. These *cis* defects correspond to a partial folding of chains, clearly visible in the insert image [partial folds located near the upper left corner of the white dotted square, in the inset image of Fig 4(b)].

#### IV. DISCUSSION

The heterogeneous nature of the P3HT film deposited on HOPG is clearly seen in the mesoscopic scale ( $\mu\text{m}$ ) images. Polycrystalline patches spanning over several hundred nanometers coexist with amorphous and/or uncovered areas. We note that it may be possible to reach the percolation threshold between polycrystalline patches by following two routes: First, in general, the exact morphology of the polymer on the mesoscopic scale can be changed in a controlled manner by varying the polymer concentration in the casting solution and/or by varying the solvent evaporation rate. Second, it can also be influenced, to some extent, by postdeposition annealing, which usually leads to an increase in the crystalline domain average size.<sup>10</sup> Studies on these two strategies are in progress.

Inside the polycrystalline areas (sub- $\mu\text{m}$  scale) monodomains have an average size  $\approx 20 \text{ nm}$  in both parallel (along the  $\pi$ -conjugated backbone) and transverse (perpendicular to the  $\pi$ -conjugated backbone) directions. Remarkably, this size is of the same order as the typical coherence lengths (in the range  $8\text{--}13 \text{ nm}$ <sup>10,11</sup>) reported from XRD measurements for thicker P3HT films. The larger value obtained in our case is consistent with epitaxial effects promoting P3HT 2D ordering with threefold symmetry on HOPG. Furthermore, adjacent monodomains with different orientations are clearly connected by folded chains. This gives direct evidence that the interfaces between P3HT domains are more complex than well-defined grain boundaries found in more simple molecular systems (model compounds) such as self-assembled  $\pi$ -conjugated oligomers.

On a more local scale, images reveal that chain conformations and packing are quite similar to those previously reported at the solution/substrate interface.<sup>17,18</sup> Especially, epitaxial effects promote full interdigitation of hexyl sidechains, resulting in a dense packing of macromolecules (the energetically most stable state on HOPG<sup>21</sup>). The chain-to-chain distance  $d_{cc} \approx 1.4 \text{ nm}$ , is then smaller than the “relaxed” value obtained in bulk samples from XRD studies [ $d_{cc} \approx 1.6 \text{ nm}$  (Ref. 11)]. Besides, chain folding occurs with a large majority (70%) of folds ( $120^\circ$  and  $60^\circ$ ) following three-fold epitaxy-induced symmetry.

Remarkably, the average chain length deduced from STM images (26 nm) is nearly equal to the value obtained from SEC measurements (29 nm). Recent studies have demonstrated<sup>14</sup> that neither shorter nor longer chains of poly-

mers in solution adsorb on the surface at equilibrium. Such a “fractionation phenomenon” may severely affect molecular weight estimation from STM images when performing measurements at the solution/substrate interface. In that sense, STM imaging of polymers at the solid/substrate interface appears as an appropriate tool for molecular weight estimation.

Last, subnanometer resolved images display modulations (along the  $\pi$ -conjugated backbone axis) corresponding to diad or triad chain periodicities (Scheme 1). The value found for the b3HT distance ( $7.6 \pm 0.2$  Å) is slightly smaller (within the error bars) than the value expected from molecular mechanics calculation<sup>19</sup> (7.8 Å). In the case of regioregular (HT-HT > 98%) poly(3-dodecylthiophene) (P3DDT), Mena-Osteritz *et al.* reported “bithiophene” chain periodicities of 6.8 Å (Ref. 17) (note that the term “bithiophene” is *a priori* equivalent to our definition of the b3HT distance). The authors calculated a bithiophene value “in the gas phase” of 7.4 Å. They explained this difference on the basis of a model of epitaxy-induced compression, in which every second thiophene matches a similar electronic environment on graphite, giving rise to a more intensive tunneling current. Interestingly, in our case, we note that in some parts of the chain backbone, individual thiophene units appear alternatively as big and small spots [Fig. 4(b)]. This indicates that P3HT epitaxy on HOPG may induce a compression effect, similar to the one previously reported for P3DDT.

Finally, within the resolution of our experiment, the visualization of thiophene repeating units (*vide supra*) allowed us to propose possible intrachain isomerism (*trans* vs *cis*) with all-*trans* geometry in linear parts and *cis* defects near folds. This matter will be the subject of further investigations. In particular, we propose achieving a better intrachain resolution, by performing low-temperature STM imaging of 2D P3HT ordered domains.

## V. CONCLUSION

We have succeeded in performing multi-scale STM analysis at the solid/substrate interface of self-organized P3HT films deposited on HOPG. From the STM images a picture emerges, where structural heterogeneities exist at different length scales. We believe that such heterogeneities (amorphous areas, interconnections and interfaces between domains, misfits, folds and intrachain *cis* conformations) may significantly affect the global electronic properties of P3HT films. This is most likely for samples with domain orientation versus substrate as in our study. Moreover, as epitaxial effects on HOPG promote polymer ordering, one may obtain higher degrees of disorder for samples grown on other substrates (such as insulating layers used in FETs).

Therefore, an issue that should be addressed in the future is the possibility to probe the electronic properties in P3HT films, when varying the typical length scales. One promising route implies local probes of the electronic transport, such as potentiometry techniques based on scanning probe microscopies.<sup>25–28</sup> Another strategy may consist in a progressive reduction of the gap distance between source and drain in FETs.

Last, we underscore that the possibility of carrying out STM studies of P3HT 2D polycrystals *at the solid/substrate interface* opens new fields of investigation, especially concerning low-temperature spectroscopic measurements and local polymer modifications with the STM.<sup>29</sup>

## ACKNOWLEDGMENTS

M. Fakir and C. Lombard are gratefully acknowledged for providing technical development and support. We thank Dr. P. Reiss for careful reading of the manuscript. This work is in part supported by “CPER Nanophysique-région Rhône-Alpes,” France.

- <sup>1</sup>R.D. McCullough and R.D. Lowe, J. Chem. Soc. Chem. Commun. **1**, 70 (1992).
- <sup>2</sup>T.A. Chen and R.D. Rieke, J. Am. Chem. Soc. **114**, 10087 (1992).
- <sup>3</sup>R.S. Loewe, P.C. Ewbank, J. Liu, L. Zhai, and R.D. McCullough, Macromolecules **34**, 4324 (2001).
- <sup>4</sup>H.E. Katz, Z. Bao, and S.L. Gilat, Acc. Chem. Res. **34**, 359 (2001).
- <sup>5</sup>Z. Bao, A. Dodabalapur, and A.J. Lovinger, Appl. Phys. Lett. **69**, 4108 (1996).
- <sup>6</sup>H. Sirringhaus, N. Tessler, and R.H. Friend, Science **280**, 1741 (1998).
- <sup>7</sup>H. Sirringhaus, P.J. Brown, R.H. Friend *et al.*, Nature (London) **401**, 685 (1999).
- <sup>8</sup>W. Fix, A. Ullmann, J. Ficker, and W. Clemens, Appl. Phys. Lett. **81**, 1735 (2002).
- <sup>9</sup>T.J. Prosa, J. Moulton, A.J. Heeger, and M.J. Winokur, Macromolecules **32**, 4000 (1999).
- <sup>10</sup>K.E. Aasmundtveit, E.J. Samuelsen, M. Guldstein *et al.*, Macromolecules **33**, 3120 (2000).
- <sup>11</sup>H. Sirringhaus, P.J. Brown, R.H. Friend, M.M. Nielsen, K. Bechgaard, B.M.W. Langeveld-Voss, A.J.H. Spiering, R.A.J. Janssen, and E.W. Meijer, Synth. Met. **111–112**, 129 (2000).
- <sup>12</sup>E.J. Samuelsen, D.W. Breiby, O. Kononov, B. Struth, and D.M. Smilgies, Synth. Met. **123**, 165 (2001).
- <sup>13</sup>S.S. Sheiko and M. Möller, Chem. Rev. **101**, 4099 (2001).
- <sup>14</sup>P. Samorí and J.P. Rabe, J. Phys.: Condens. Matter **14**, 9955 (2002).
- <sup>15</sup>E. Lacaze, K. Udval, P. Bodö, J. Garbarz, W.R. Salaneck, and M. Schott, J. Polym. Sci., Part B: Polym. Phys. **31**, 111 (1993).
- <sup>16</sup>K. Kaneto, K. Harada, W. Takashima, K. Endo, and M. Rikukawa, Jpn. J. Appl. Phys. Part 2 **38**, L1062 (1999).
- <sup>17</sup>E. Mena-Osteritz, A. Meyer, B.M.W. Langeveld-Voss, R.A.J. Janssen, E.W. Meijer, and P. Bäuerle, Angew. Chem. Int. Ed. Engl. **39**, 2680 (2000).
- <sup>18</sup>E. Mena-Osteritz, Adv. Mater. **14**, 609 (2002).
- <sup>19</sup>H. Kasai, H. Tanaka, S. Okada, H. Oikawa, T. Kawai, and H. Nakanishi, Chem. Lett. 696 (2002).
- <sup>20</sup>T. Hassenkam, D.R. Greve, and T. Bjørnholm, Adv. Mater. **13**, 631 (2001).
- <sup>21</sup>S. Yin, C. Wang, X. Qiu, B. Xu, and C. Bai, Surf. Interface Anal. **32**, 248 (2001).
- <sup>22</sup>S. Holdcroft, J. Polym. Sci., Part B: Polym. Phys. **29**, 1585 (1991).
- <sup>23</sup>T. Yamamoto, D. Oguro, and K. Kubota, Macromolecules **29**, 1833 (1996).
- <sup>24</sup>J. Liu, R.S. Loewe, and R.D. McCullough, Macromolecules **32**, 5777 (1999).
- <sup>25</sup>K. Seshadri and C.D. Frisbie, Appl. Phys. Lett. **78**, 993 (2001).
- <sup>26</sup>L. Bürgi, H. Sirringhaus, and R.H. Friend, Appl. Phys. Lett. **80**, 2913 (2002).
- <sup>27</sup>B. Grévin, I. Maggio-Aprile, A. Bentzen, L. Rannot, A. Llobet, and Ø. Fischer, Phys. Rev. B **62**, 8596 (2000).
- <sup>28</sup>B. Grévin, I. Maggio-Aprile, A. Bentzen, O. Kuffer, I. Joumard, and Ø. Fischer, Appl. Phys. Lett. **80**, 3979 (2002).
- <sup>29</sup>Y. Okawa and M. Aono, J. Chem. Phys. **115**, 2317 (2001).
- <sup>30</sup>R. Fernández *et al.*, WSXM Version 3.0 (Nanotec Electronica, Madrid, Spain) (www.nanotec.es).